Smart Structures and Systems, *Vol. 11, No. 5 (2013) 477-496*
DOI: http://dx.doi.org/10.12989/sss.2013.11.5.477

Develoment of high-sensitivity wireless strain sensor for structural health monitoring

Hongki Jo[1], Jong-Woong Park[2], B.F. Spencer, Jr.[*1] and Hyung-Jo Jung[2]

[1]*Department of Civil and Environmental Engineering, UIUC, Urbana 61800, USA*
[2]*Department of Civil and Environmental Engineering, KAIST, Daejeon 305-701, Korea*

(Received June 11, 2012, Revised November 25, 2012, Accepted November 30, 2012)

Abstract. Due to their cost-effectiveness and ease of installation, wireless smart sensors (WSS) have received considerable recent attention for structural health monitoring of civil infrastructure. Though various wireless smart sensor networks (WSSN) have been successfully implemented for full-scale structural health monitoring (SHM) applications, monitoring of low-level ambient strain still remains a challenging problem for WSS due to A/D converter (ADC) resolution, inherent circuit noise, and the need for automatic operation. In this paper, the design and validation of high-precision strain sensor board for the Imote2 WSS platform and its application to SHM of a cable-stayed bridge are presented. By accurate and automated balancing of the Wheatstone bridge, signal amplification of up to 2507-times can be obtained, while keeping signal mean close to the center of the ADC span, which allows utilization of the full span of the ADC. For better applicability to SHM for real-world structures, temperature compensation and shunt calibration are also implemented. Moreover, the sensor board has been designed to accommodate a friction-type magnet strain sensor, in addition to traditional foil-type strain gages, facilitating fast and easy deployment. The wireless strain sensor board performance is verified through both laboratory-scale tests and deployment on a full-scale cable-stayed bridge.

Keywords: structural health monitoring; wireless smart sensor; high-sensitivity strain sensor; full-scale deployment

1. Introduction

Catastrophic structural failures in recent years have attracted public attention to the declining state of aging civil infrastructure and the necessity for Structural Health Monitoring (SHM). The research community has turned to Wireless Smart Sensor Networks (WSSN) over traditional wired system to develop approaches for monitoring the health of essential infrastructure, both old and new. WSSNs offer many attractive features, such as ease of installation, wireless communication, on-board computation, battery-power, relatively low cost, and small size. Indeed, SHM using wireless smart sensor technology has emerged as a promising solution that can reduce inspection costs, optimize repairs, and ensure public safety as building and bridge structures get higher, longer, and more complex. Recent successful implementations of various WSSNs for full-scale SHM systems have demonstrated the practical use of the technology (Jang *et al*. 2010, Cho *et al*.

*Corresponding author, Professor, E-mail: bfs@illinois.edu

http://www.techno-press.org/?journal=sss&subpage=5 ISSN: 1738-1584 (Print), 1738-1991 (Online)

2010, Kurata *et al*. 2010, Whelan *et al*. 2010, Zonta *et al*. 2010, Meyer *et al*. 2010, Spencer and Cho 2011). However, despite these successful implementations, strain monitoring, particularly low-level ambient dynamic strain monitoring, is still a challenging problem using wireless smart sensors (WSS) due to A/D converter (ADC) resolution, inherent circuit noise, and the need for automatic operation. These problems are exacerbated by the need for accurate synchronization and high-throughput communication.

Several researchers have developed strain sensor boards for various smart sensor platforms. Nagayama *et al*. (2004) and Choi *et al*. (2008) have developed a prototype strain sensor board for MEMSIC's Mica2 platform (2007). Similarly, O'Connor *et al.* (2010) developed a board for the Narada wireless sensor (Swartz *et al*. 2005). However, the applicability of these basic-functioning strain sensor boards to low-level ambient strain is limited. For example, Whelan and Janoyan (2009) and Bischoff *et al*. (2009) have designed a signal conditioning board for Tmote Sky platform (Moteiv 2006) using the ZMD31050 differential sensor signal conditioner (ZMD 2004).

While the ZMD31050 signal conditioner features digitally programmable analog offset nulling, the approach to offset removal (i.e., by adding an analog voltage to the signal) restricts the gain to a maximum of only 420, which is not sufficient for sub-micro strain levels. Commercial wireless strain sensors are recently available (Microstrain 2011, National Instrument 2010); however, these nodes either: (i) emulate wired monitoring systems, or (ii) act as simple data loggers. Neither of these approaches are scalable, and thus do not allow for dense instrumentation of large civil infrastructure; moreover, they are primarily intended for short-term monitoring campaigns.

This study presents a new WSS strain sensor board (SHM-S) using MEMSIC's Imote2 WSS platform that enables easy and precise strain monitoring of steel structures. Following a description of the hardware design and associated software, the SHM-S/Imote2 is experimentally validated in the laboratory for traditional foil-type strain gages, as well as magnet-type friction strain sensor (Tokyo Sokki 2005). Automated, precise balancing of the Wheatstone bridge is shown to facilitate signal amplification of up to 2507; this level of gain is sufficient for low-level ambient strain monitoring. An onboard shunt calibrator allows for very simple calibration of the strain circuit, and an optional half-bridge circuit is also provided for temperature compensation.

The SHM-S/Imote2, combined with the magnet strain sensor, enables fast and easy installation of strain sensors on steel structures without requiring cumbersome installation of the strain gages (i.e., paint removal, surface polishing, gage application). Furthermore, because the strain sensor board has been designed for combined use with the existing accelerometer board (SHM-A/ISM400) and data acquisition board (SHM-DAQ) previously developed for Imote2 WSS platform under the Illinois Structural Health Monitoring Project (ISHMP), synchronized multimetric strain sensing with acceleration or other measurands is available. Finally, the efficacy of the SHM-S/Imote2 nodes is then demonstrated for wireless strain monitoring system of a full-scale cable-stayed bridge having steel-deck and steel-pylons.

2. Development of high-precision strain sensor

2.1 Consideration for strain sensor board design

The first step in the design of a high-precision wireless strain sensor board is to secure sufficient signal amplification, as strain responses are generally just a few micro-strain (μstrain) for the ambient vibration of civil infrastructures. For example, consider a foil type 350-ohm strain

gage having gage factor of 2; if the maximum level of strain is 1~2 μstrain, then the maximum, corresponding resistance change in the strain gage is just 0.0007~0.0014 Ω. To convert the changes in resistance of the strain gage into a measurable voltage, a Wheatstone bridge circuit is generally used, and then signal amplification is required to resolve such low-level signal variations.

Considering that a 12~16bits ADC is generally adopted in wireless sensors for power efficiency and that the effective number of bit (ENOB) of the ADC is less than the specified resolution, signal amplification of several hundreds or thousands may be required. One of most critical factors for successful use of a Wheatstone bridge combined with a signal amplifier is that the bridge circuit should be precisely balanced so that the signal is zero in the nominal state (i.e., equilibrium). If accurate balancing is not achieved (e.g., due to errors in resistance values of bridge arms or strain gage), then a non-zero offset will result, which when amplified, can easily saturate the A/D of the data acquisition system. Offset nulling of amplified signal by adjusting the reference voltage of the amplifier would be one way to remove the non-zero offset effect. However, considering the available voltage range in WSS powered by batteries is quite limited, such an offset nulling approach may not be appropriate for the case for which high signal amplification is required.

Therefore accurate bridge balancing is critical prior to signal amplification.

A second issue for accurate strain sensing is temperature compensation. Though some types of strain sensors provide temperature compensated measurements, most foil-type metal strain gages still have quite high thermal sensitivity (e.g., on the order of 10 μstrain/°C). Temperature compensation is a practical issue to be addressed in real-world applications, is particularly important for cases involving large temperature changes or long-term measurements. Post compensation is possible by measuring temperature and using a correction curve provided by the manufacturers, however measuring the temperature of the structural element under consideration is not straightforward. A half-bridge circuit with a dummy gage can be used for correcting possible drift in the strain signal due to temperature changes.

Another practical issue to be considered for full-scale applications is strain sensor calibration.

Considering that conditions at site are different from laboratory or shop conditions, prior calibration parameters may not be effective once installed at the site. Therefore embedded self-calibration capability is essential for broader application of strain sensing on full-scale structures. Shunt calibration verifies the output of the strain measurement system relative to a predetermined mechanical strain. This prodedure involves simulating the predetermined strain input by shunting a known value of large resistor across the bridge arm connected to the strain gage, measuring the change of the output voltage, and estimating the sensitivity of the voltage output to the strain change.

Finally, compatibility of the strain sensor with other sensors in a WSSN is important. For the Imote2 WSS platform, several sensor boards have been developed: SHM-A accelerometer board (Rice *et al*. 2010), SHM-DAQ data acquisition board (Jo *et al*. 2011), and SHM-H high-sensitivity accelerometer board (Jo *et al*. 2012). All of those sensor boards use the same ADC, which is the Quickfilter QF4A512, a versatile 4-channel ADC and programmable signal conditioner with user-selectable sampling rate and programmable digital filters. Fig. 1 shows the functional block diagram of the Quickfilter QF4A512. Design of the new strain sensor board using the same ADC platform will make available the services previously developed for the Imote2 (see ISHMP Services Toolsuite, Rice *et al*. 2010), including synchronized sensing and reliable communication.

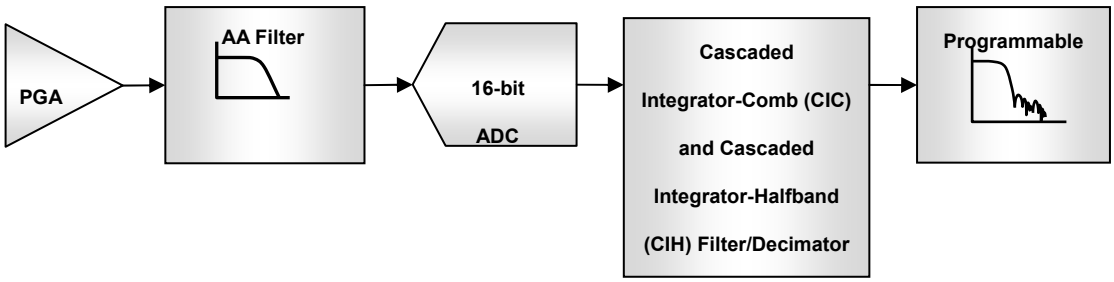

Fig. 1 Functional block diagram of Quickfilter QF4A512

2.2 Precisely balanceable Wheatstone bridge

Consider the balanced Wheatstone quarter-bridge circuit shown in Fig. 2, which is composed of 4 resistive arms with an excitation voltage (V_{EXT}) applied across the bridge circuit. Three resistive arms have the same constant resistance R, while the other arm is an active resistor of value $R + \Delta R$, where ΔR is the resistance change proportional to strain change.

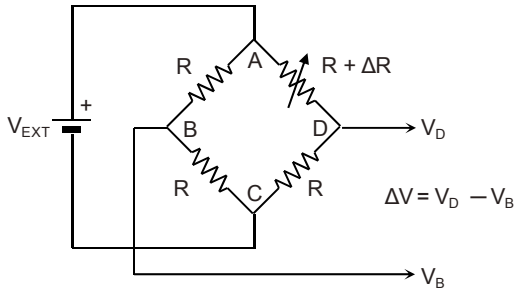

Fig. 2 Wheatstone quarter-bridge circuit

If the active resistor is a strain gage for which the gain factor $GF = (\Delta R / R)/\varepsilon$, where ε is strain, the output voltage becomes

$$\Delta V = \left[\frac{-\Delta R}{4R+2\Delta R}\right] \cdot V_{\mathrm{EXT}} = -\frac{GF\cdot\varepsilon}{4}\left[\frac{1}{1+\frac{\mathrm{GF}\cdot\varepsilon}{2}}\right] \cdot V_{\mathrm{EXT}} \approx -\frac{GF\cdot\varepsilon}{4} \cdot V_{\mathrm{EXT}} = -\frac{\Delta R}{4R} \cdot V_{\mathrm{EXT}}. \quad (1)$$

Considering actual strain measurement ε is typically only a few micro-strain for ambient vibration and the gain factor of many of typical metal foil type strain gage GF is roughly 2~5, the nonlinear term of $(GF \cdot \varepsilon)/2$ in the denominator of the third term of Eq. (1) is negligible. Then the output voltage (ΔV) from the quarter-bridge is approximately proportional to the strain (ε), consequently resistance change (ΔR) of the strain gage as shown in the last two terms of Eq. (1).

As mentioned in previous section, signal amplification from hundreds to thousands is required to measure sub-micron level ambient strain. However, if the Wheatstone bridge is not accurately balanced, any possible error in resistance values of bridge arms or strain gage can cause the bridge unbalance, which results in significant drift error in the output voltage after amplification and saturation of the ADC. For example, even a 1~2 ohm error in one of 350-ohm resistors or strain gage can cause 4.1~8.2 V signal drift after 2000 times signal amplification, which exceeds the input range on the ADC used for wireless sensors.

To balance the bridge, the new strain sensor board (SHM-S board) uses a 2-channel non-volatile digital potentiometer (MAX5479 with 256-taps 100-kohms, MAXIM 2006).

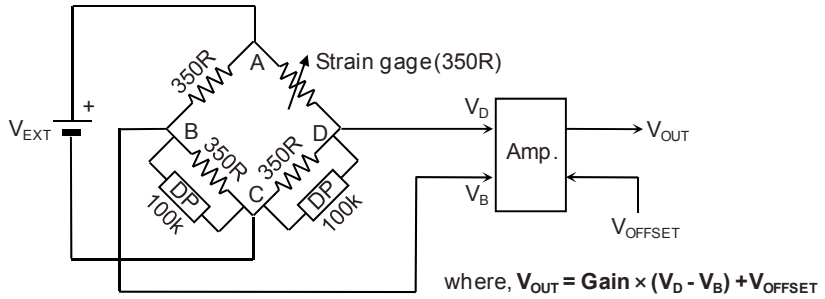

Fig. 3 Adjustable-balance Wheatstone bridge and instrumentation amplifier circuit

By connecting the 100-kohm digital potentiometer (DP) across the two of 350-ohm resistive bridge arms (see Fig. 3), very accurate resistance adjustment, up to 0.0048ohm can be achieved. And use of a digital potentiometer allows software-controllable bridge balancing. The non-volatile memory on the potentiometer allows the wiper locations to be saved to the internal EEPROM, avoiding loos of the balanced condition power cycling. For the SHM-S board, a variable-gain precision instrumentation amplifier (MAX4194, MAXIM 2003) is selected that supports single-voltage supply operation (2.7~7.5V), high gains (1~10000 times), and low-power consumption (93uA). The gain of the MAX4194 is determined by connecting a single external gain resistor and given by

$$Gain = 1 + \frac{50\text{k}\Omega}{R_\text{G}}, \tag{2}$$

where R_G is the gain-setting resistor. For the SHM-S board, four different gains of 501, 1001, 2007, and 2507 are set by connecting four values of R_G which are obtained by four different parallel combinations of two 100-ohm and one 33.2-ohm resistors with a software controllable switch. The final output voltage from the amplifier is determined by multiplying the difference of the differential inputs (V_D and V_B in Fig. 3) by the gain obtained from Eq. (2) and adding the reference/offset voltage (V_OFFSET in Fig. 3) as follows

$$V_\text{OUT} = Gain \times (V_\text{D} - V_\text{B}) + V_\text{OFFSET}. \tag{3}$$

2.3 Temperature compensation and shunt calibration

Use of the half-bridge configuration with a dummy strain gage is one way to reduce the temperature effect. For all strain gages in a bridge at the same temperature and mounted at the same location, any change in temperature affects all gages in the same way. Therefore, the use of a dummy gage in the half-bridge configuration allows compensating the signal drift in the counter-part active gage due to the temperature change. Of course, the half-bridge option can be used to double the sensitivity of the bridge to strain with active strain gages for both arms. In the SHM-S board, the half-bridge configuration is user-selectable and even can be deactivated, which then becomes a quarter-bridge configuration, with an analog switch (switch 2 in Fig. 4).

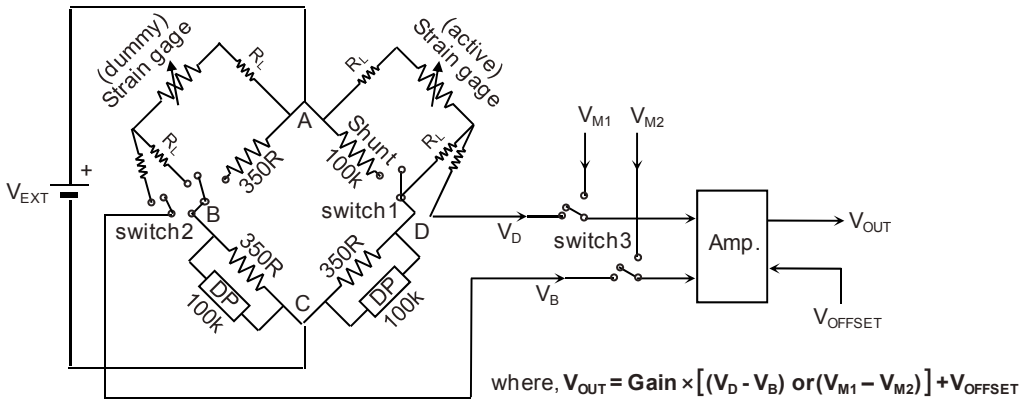

Fig. 4 Strain bridge circuit including both temperature compensation and shunt calibration

For shunt calibration, the SHM-S board employed a high-precision 100-Kohm resistor having 0.1% tolerance error and a software-controllable switch (switch 1 in Fig. 4). For the 350-ohm strain gage, connection of the 100-Kohm resistor across the strain gage results in about 1.221 ohm reduction in resistance, which corresponds to the strain input of about 1676.8 μstrain with GF = 2.08 (the GF = 2.08 is for the 350-ohm foil-type strain gage to be used subsequently for verification experiments).

2.4 Magnetic strain sensor

One of the disadvantages of strain measurements using the foil type strain gages is that the gage installation process is time consuming and can be difficult in the field. As an alternative, Tokyo Sokki Kenkyujo (2005) has released a strain checker (FGMH-1) which is a non-destructive-type strain sensor composed of a frictional strain gage and magnet attachment (see Fig. 5).

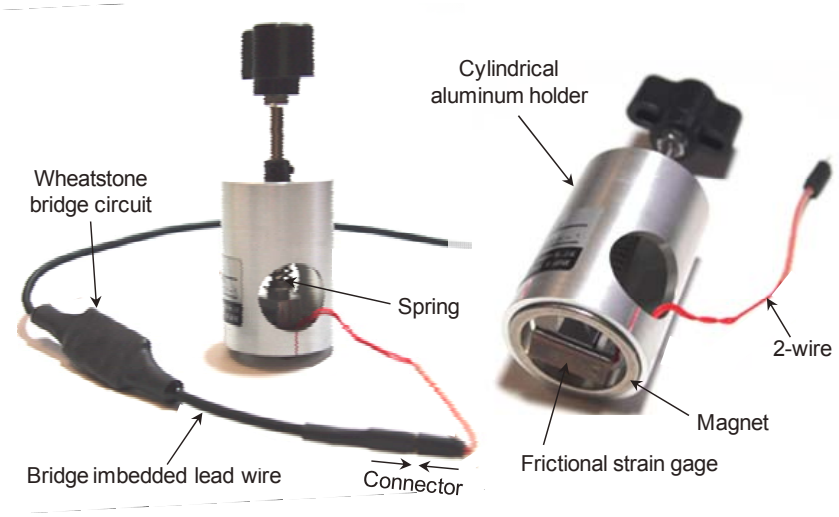

Fig. 5 Friction-type magnet strain sensor (FGMH-1, Tokyo Sokki 2005)

While ordinary strain gages measure the strain through adhesive, the strain checker employs a cylindrical magnet which secures the aluminum holder to steel structure; a spring inside the holder press the strain gage onto the steel surface (see Fig. 5). Because the base plate in which the 122-ohm strain gage is embedded, which will directly touch the surface, is coated by emery powder, the strain can be measured by friction (O'Brien *et al*. 2008). With the strain checker, adhesives are not required; strain measurements even can be made without removing the paint of the structure. Combining the FGMH-1 with the SHM-S/Imote2 WSS node offers a powerful tool for investigating the performance of steel structures.

SHM-S board has been designed to properly interface with the magnet strain checker. Because the strain checker comes with a Wheatstone-bridge embedded lead wire (left of Fig. 5), the differential voltage signals from the strain checker system needs to be fed to the amplifier directly. By putting another analog switch (switch 3 in Fig. 4) on the SHM-S board for bypassing the bridge of the board, direct use of the amplifier is possible.

2.5 Compatibility with other previous sensor boards

The SHM-S board has been designed to be stackable on the SHM-A accelerometer board or SHM-DAQ data acquisition board to utilize the ADC on the boards. The first three channels of the QF4A512 ADC on the SHM-A board are connected to the 3-channels MEMS accelerometer and the other 4th channel is left to accommodate an external analog sensor, which is used by the SHM-S board. For the SHM-DAQ board, all four channels are open to external analog input; for convenience, the strain signal from the SHM-S board is connected to the 1st channel of the SHM-DAQ board. An important advantage of the SHM-S board by using the same ADC as the SHM-A and SHM-DAQ boards is that it can fully utilize all functions of the SHM boards and ISHMP Services Toolsuite based network.

Fig. 6 shows the block diagram of the SHM-S board, and Fig. 7 shows the SHM-S board stacked on the SHM-A (left) and on the SHM-DAQ board (right).

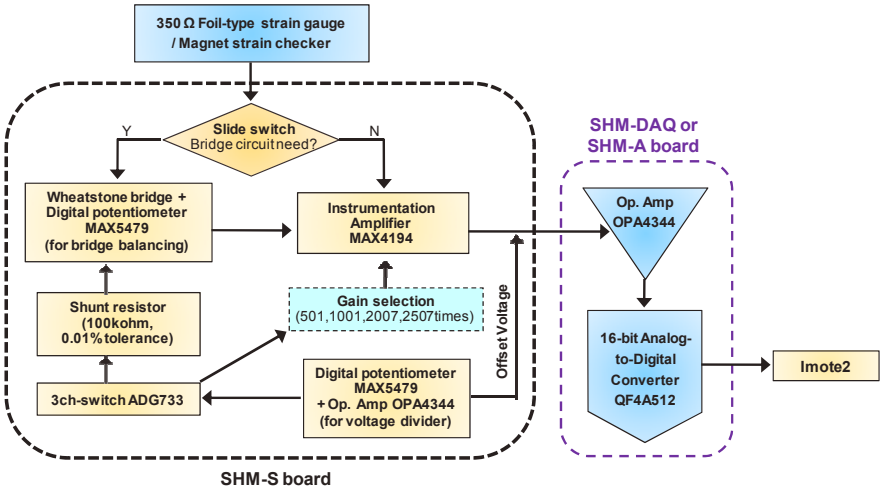

Fig. 6 Block diagram of SHM-S board

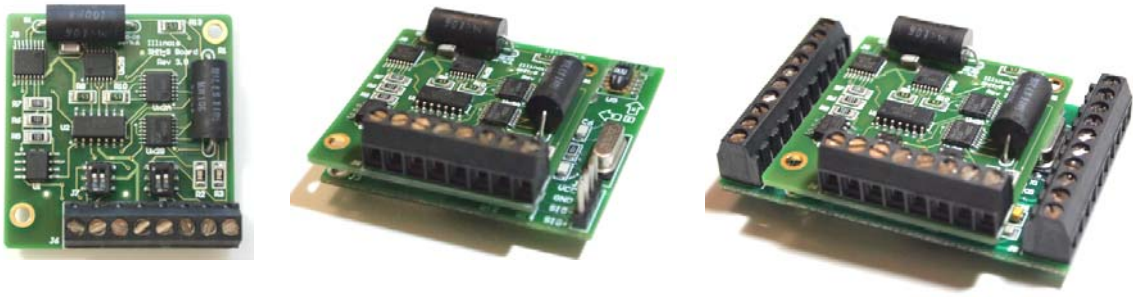

Fig. 7 SHM-S board (left): stacked on SHM-A (middle) and on SHM-DAQ board (right)

3. Software design for strain sensor board

3.1 ISHMP Services Toolsuite

The Illinois Health Monitoring Project (ISHMP) has developed an open-source software framework based on the design principles of service-oriented architecture (Rice *et al*. 2010). The framework provides a software library of customizable services for SHM applications using the Imote2, implementing the key middleware infrastructure necessary for high-quality sensing, including: various low-level foundation services for synchronized and reliable network operation, as well as high-level application services, tools, and utilities. Some key service modules employed in this study include:

- *ReliableComm*[*] – for reliable wireless communication of both short messages and long data records
- *SensingUnit* – flexible network-wide synchronized sensing service
- *RemoteSensing* – fault tolerant implementation of the *SensingUnit* service for time synchronization, wireless sensing, and storing the data to Flash memory
- *RemoteCommand* – service that supports the reliable dissemination of network commands

3.2 Autonomous bridge balancing and calibration

To effectively use the SHM-S board in the Imote2 based sensor network, software for autonomous bridge balancing and shunt calibration (*SHMSAutoBalance*; see Fig. 8) was developed using the ISHMP Services Toolsuite. The software operates to check the signal output offset and then compensates the signal output offset to a designated level. The SHM-S board supports two methods of signal output offset compensation (i.e., zero shift): 1) reference voltage shift after signal amplification and 2) bridge balance control before signal amplification. If the offset error of the amplified signal is too large (i.e., beyond the output range (0~3V) of the (MAX4194) amplifier), it will be saturated at the top or bottom limit. In this case, the deviant signal needs to be guided by adjusting the reference voltage for the amplifier so that it will be in the range for which the bridge balancing process can work. Once the output voltage is in the proper range, then the bridge balancing process is carried out by adjusting the resistance of the digital potentiometers connected across the bridge arms, as shown in Figs. 3 and 4. This two-step compensation procedure allows an accurate zero shift up to 200% of the processible signal span.

Once the signal-offset error compensation process is complete, the shunt calibration process is conducted. By connecting the shunt resistor across the bridge arm using a programmable switch, a known-value of strain input is simulated. Then the ratio of the voltage change due to the simulated strain input to the amount of strain input is the sensitivity, which is used to convert the voltage output to physical strain units.

Fig. 8 shows the simplified block diagram for the software (*SHMSAutoBalance*); detailed procedures for the autonomous bridge balancing and shunt calibration using the ISHMP Services Toolsuite are as follows:

1) Gateway node send a set of default parameters to a leaf sensor node using *ReliableComm*; i.e., minimum gain, default wiper position of the potentiometer and reference voltage of the amplifier, and sensing parameters.
2) Short-term sensing started in the leaf node using *SensingUnit* with the parameters received.
3) Mean of the voltage output measurement calculated.
4) If the voltage mean is larger than upper limit or less than lower limits, then adjust the reference voltage of the amplifier.
5) If the mean voltage, after (4) is carried out, is in the proper range, check if the mean is larger than default reference voltage.
6) If the mean voltage is larger than the reference voltage, adjust the resistance of the potentiometer connected across CD in Figs. 3 and 4 to balance the bridge. Otherwise, adjust the potentiometer across BC.
7) Check the output mean voltage after short-term sensing with the balanced bridge.

[*] Use of the *Italic font* designates a tool or service name in the ISHMP Services Toolsuite.

8) Connect the shunt resistor and begin sensing.
9) Compare the mean voltages of (8) with (7), find the sensitivity of the output voltage to the strain, and send it to the gateway node.
10) Disconnect the calibration resistor from the bridge, and set new gain for actual sensing.

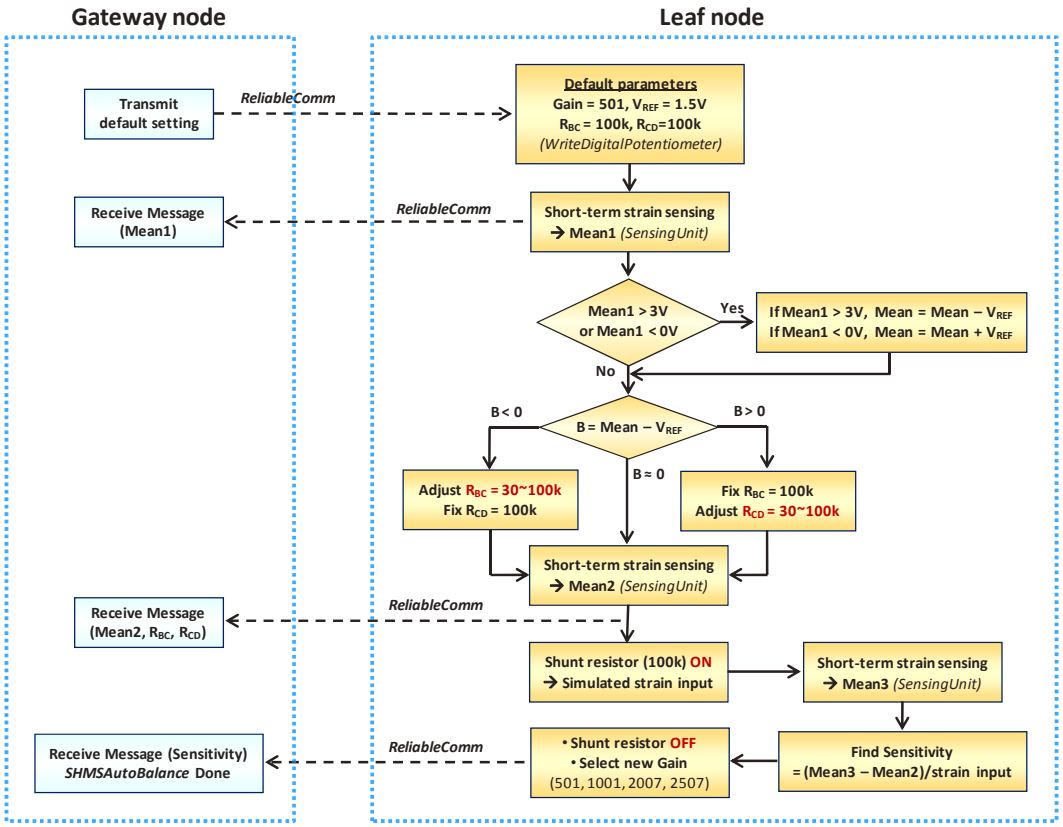

Fig. 8 Block diagram of *SHMSAutoBalance* service in the ISHMP Services Toolsuite

4. Validation of the high-precision strain sensor board

The performance of the developed wireless strain sensing system on the SHM-S board and the associated software has been verified through lab-scale tests. Strain measurements using the wireless strain sensing system are compared with a conventional wired system. The National Instrument (NI) DAQ system with SCXI-1520 universal strain gage input module combined with a SCXI-1314 front-mounting terminal block was used for the wired measurements (National Instrument 2007a,b). For this test, a one-bay 3-story shear building having steel-plate columns was used (see Fig. 9, left). Two foil-type 350-ohm strain gages with GF = 2.08 and the magnet strain checker (FGMH-1) were attached on the exterior surface of the column around the 2nd floor (see Fig. 9, right). To check the performance of the SHM-S board in both the high-level and low-level

strain range, long-time impulse responses were measured. Once an impulse load is applied to the structure, free vibration was measured until it approaches 1~2 μstrain level. The strain response measurement using the SHM-S board was compared with the one measured by the NI-DAQ for two different cases in both the time and frequency domain:

- Case 1: SHM-S board with foil-type strain gage vs. Ni-DAQ (with AA filter of 10 Hz cut-off) with foil-type strain gage.
- Case 2: SHM-S board with magnet strain checker vs. Ni-DAQ (with AA filter of 10 Hz cut-off) with foil-type strain gage.

A 100 Hz sampling rate was used for both wireless and wired system. The SHM-DAQ board was used to provide ADC (QF4A512) capability for the SHM-S board; a low-pass digital filter with a 30 Hz cut-off, and a 100 Hz sampling rate was set.

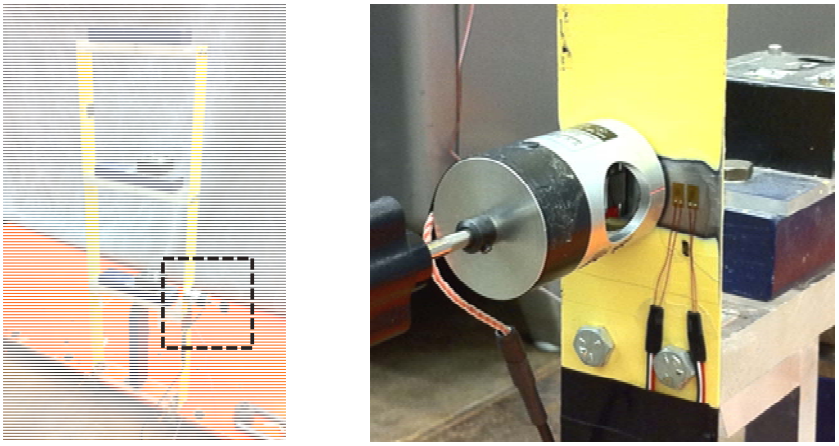

Fig. 9 Strain sensor performance test using 3-story shear building

4.1 SHM-S board with foil-type strain gage (Case 1)

The synchronized strain impulse responses for the Case 1 are shown in Fig. 10. The response starts from about ±40 μstrain initial amplitude, tapering to close to ±1.0 μstrain after 200 seconds, as shown in Fig. 10(a). Three natural frequencies of 0.879 Hz, 2.637 Hz, and 4.004 Hz were clearly found in the power spectral densities (PSD) of both the wired and wireless measurement (see Fig. 10(b)). Fig. 10(c) shows that the wireless and wired measurements are well matched at high strain levels. In Fig. 10(d), even for low-level strains of ±1.0 μstrain, both measurements show quite good agreement, though some noise and quantization are observed on the order of 0.2 μstrain.

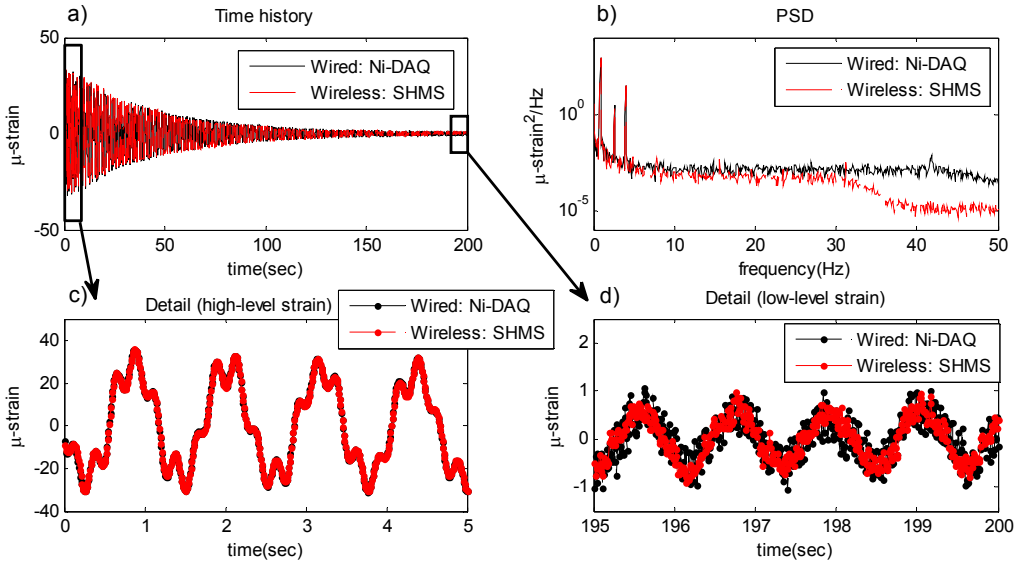

Fig. 10 Strain impulse response, Case 1: Ni-DAQ with a foil-type strain gage (with AA filter of 10 Hz cutoff) vs. SHM-S board with a foil-type strain gage

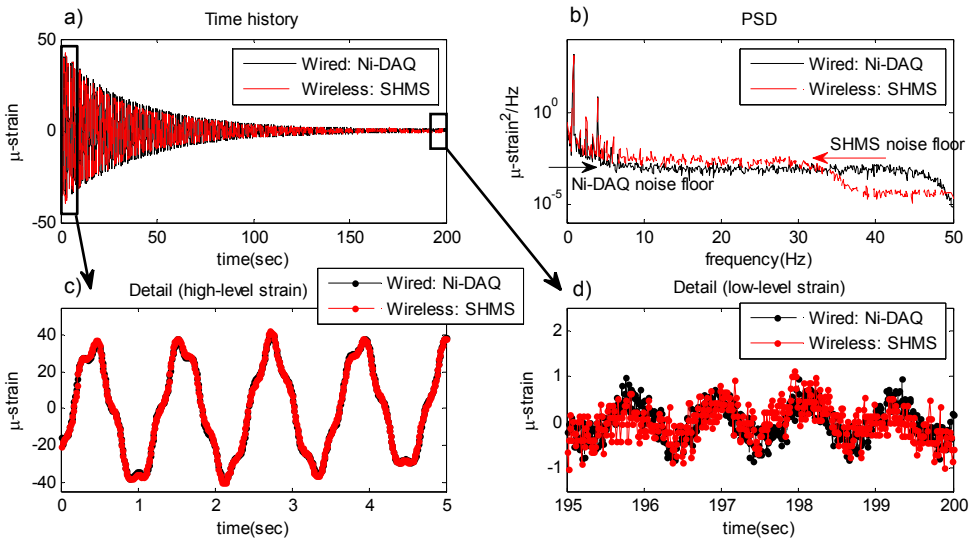

Fig. 11 Strain impulse response, Case 2: Ni-DAQ with a foil-type strain gage (with AA filter of 10 Hz cutoff) vs. SHM-S board with a magnet strain checker

4.2 SHM-S board with magnet strain checker (Case 2)

The performance of the magnet strain checker combined with the SHM-S board also has been compared with the NI-DAQ system. For this test, the bridge imbedded in the lead wire for the strain checker was used and the differential signals from the strain checker system were directly connected to the amplifier, bypassing the Wheatstone bridge of the SHM-S board. As shown in Fig. 11, the performance of the magnet strain checker was excellent at high strain levels (see Fig. 11(c)). However, the magnet strain checker measurement was slightly noisier than the wired sensor at low-level strains, (see Fig. 11(d)). One can see that the measurement by the magnet strain checker is noisier in frequency domain as well; the noise floor of the magnet strain checker is a bit higher than the one for NI-DAQ over entire frequency (see Fig. 11(b)). For such low strain levels, a foil strain gage adhered in the traditional manner performed better than magnet strain checker using the friction interface.

5. Strain monitoring of a cable-stayed bridge

The wireless strain sensing system was deployed on the Jindo cable-stayed bridge in Korea. The purposes of this deployment were two-fold: 1) the performance evaluation of the wireless strain sensing system in the field and 3) the strain characteristic estimation of a three-span steel-box-girder cable-stayed bridge.

5.1 Jindo bridge

As a collaborative project between the University of Illinois at Urbana-Champaign (USA), KAIST (Korea), and the University of Tokyo (Japan), the SHM system using ISHMP based WSSN has been deployed on a cable-stayed bridge (the 2nd Jindo Bridge) in Korea (Jang *et al*. 2010, Cho *et al*. 2010, Jo *et al*. 2011). The Jindo Bridges are twin cable-stayed bridges, which connect Jindo Island and the southwest tip of Korean peninsula near the town of Haenam. The subject of this project is the 2nd Jindo Bridge, which was constructed in 2006 (left bridge in Fig. 12). The bridge is a three-span, steel-box-girder, cable-stayed bridge composed of 344 m of main span and two 70 m-length side spans. The streamlined steel-box girder is supported by the sixty stay cables connected the two A-shaped steel pylons founded on concrete piers.

Fig. 12 Jindo Bridges (left is the 2nd Jindo Bridge with wireless monitoring system)

The most recent deployment in 2010 includes total 669 channels of acceleration, temperature, humidity, light, and wind with 113 sensor nodes in four sub-networks. Two base stations were used, one for the Haenam and one for the Jindo side networks, with each of them including two gateway nodes (for deck and cable networks). All sensor nodes are equipped with solar power energy harvesting systems. Several services from the ISHMP Services Toolsuite were employed, including: *AutoMonitor* for autonomous network operation, *ChargerControl* for energy harvesting and power management, *ThresholdSentry* for triggering based network activation, and *SnoozeAlarm* for power management using sleep mode, network *AutoUtilCommand* for status monitoring, and *RemoteSensing* for synchronized wireless data acquisition. In addition, *CableTensionEstimation* was used for acceleration-based decentralized cable tension force estimation, and *DecentralizedDataAggregation* was used for decentralized data acquisition, which reduces wireless communication and consequent power consumption. Finally, a multihop communication protocol was used for one of the sub-networks, and diverse fault tolerant and power efficient features were implemented for stable long-term operation of the WSSN. Fig. 13 shows the sensor topology of the 2nd Jindo Bridge SHM system. In this deployment, the wireless strain sensing system combined with foil-type strain gages was installed only on the Haenam-side pylon to see the long term performance, and the campaign-type (short-term) sensing with magnet strain checker was used for girder strain monitoring only at the mid-span and the girder around Haenam-side pylon-bearing location.

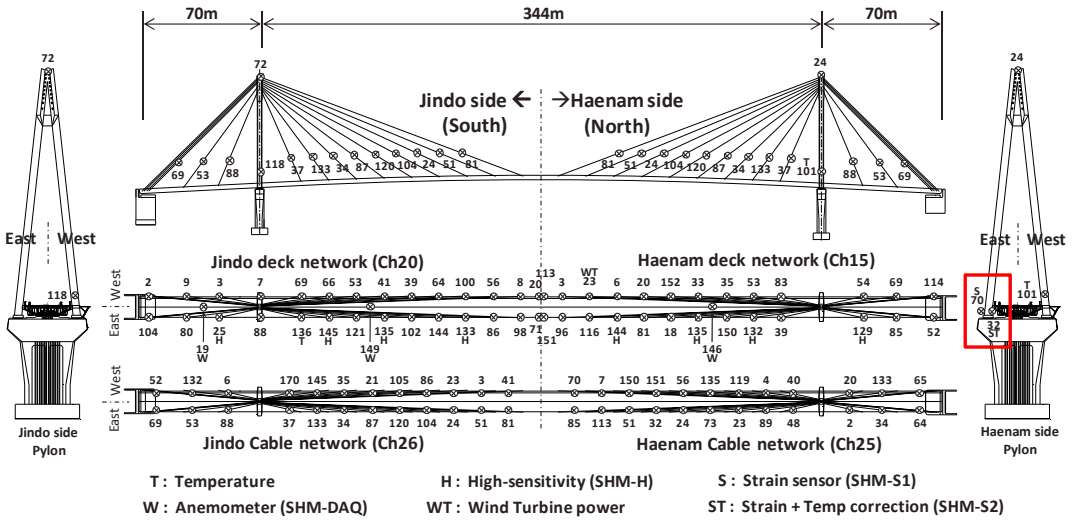

Fig. 13 Sensor topology with node IDs of the 2nd Jindo Bridge SHM system

5.2 Strain sensing on the Jindo bridge pylon

The newly developed wireless strain sensing system was installed on the lower part of Haenam-side steel pylon (node ID 70 and 32 in the Haenam-side pylon of Fig. 13). Traditional foil-type 350-ohm strain gages were used and connected to the SHM-S boards. Because the bridge

 ISSN: 1738-1584 (Print), 1738-1991 (Online)

is located in a coastal area with a corrosive environment, removing the exterior paint of the bridge for strain gage installation was not allowed. So the strain gages were installed inside the pylon to measure pylon strain in the vertical direction (left of Fig. 14) and wired to the strain sensor nodes located outside the pylon (right of Fig. 14). Among the two strain nodes, only one sensor node (node ID 32) used the half-bridge option with a dummy strain gage for temperature compensation. The SHM-S board was stacked on the SHM-A board for multi-metric sensing of both acceleration and strain in synchronized manner (i.e., tri-axial acceleration in the first three channels and strain in the fourth channel). The Wheatstone bridge of the strain sensor board is balanced after installation; subsequently, the gain of the amplification was increased to 2007 times.

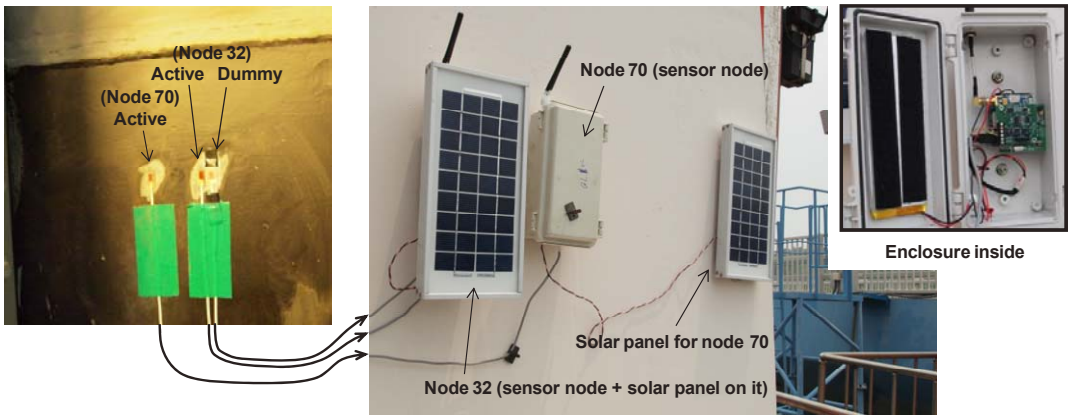

Fig. 14 Strain gages inside pylon (left) and sensor nodes outside pylon (right)

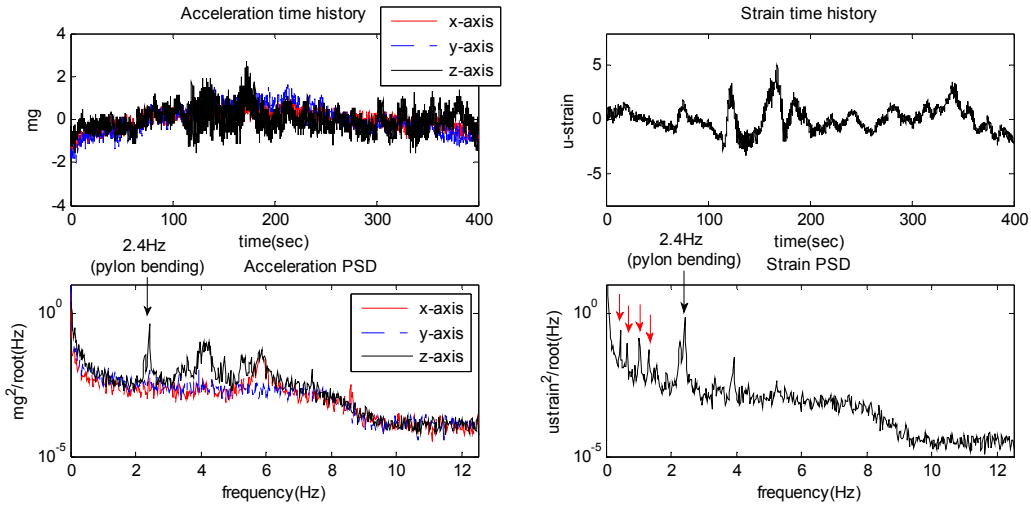

Fig. 15 Example of synchronized acceleration (left) and strain measurements (right) on pylon

The results for the acceleration and strain measurements on the pylon, 400 seconds of data at 25 Hz sampling rate, are shown in Fig. 15. The acceleration levels for the three-axes acceleration measurements are about 2 mg and strain level was -3~5 μstrain, corresponding to quite low level of vibration. As shown in the PSDs of Fig. 15, only the z-axis (i.e., longitudinal direction of the bridge) acceleration PSD shows meaningful mode around 2.4 Hz (the 1st pylon bending mode, Cho *et al*. 2010). Additionally, the strain measurements provide more information in the low frequency range, showing four distinct peaks below 2 Hz, corresponding to the 1st ~ 4th girder bending modes.

The proposed wireless strain sensing system functioned well for ambient vibration monitoring for this cable-stayed bridge; the strain measurement was even more informative than acceleration measurements in the low frequency region.

To check the performance of the temperature compensation method using the half-bridge configuration with a dummy strain gage, mean values of the series of strain measurements at different time are compared in Fig. 16. Once the Wheatstone bridge of the SHM-S board was balanced on September 21th, the strains were measured over three weeks without changing the bridge balance. A sensing event was activated only when the structural responses exceed a certain level specified by *AutoMonitor* and *ThresholdSentry*. As a result, the times of the measurements were random. Fig. 16 shows the mean strains, which should be zero and can be viewed as representing strain drift due to temperature; a clear difference is observed between the compensated and uncompensated configurations. While the strain measurement at node 70 using the quarter-bridge option shows significant drifts over three weeks, node 32 data with temperature compensation is quite well balanced.

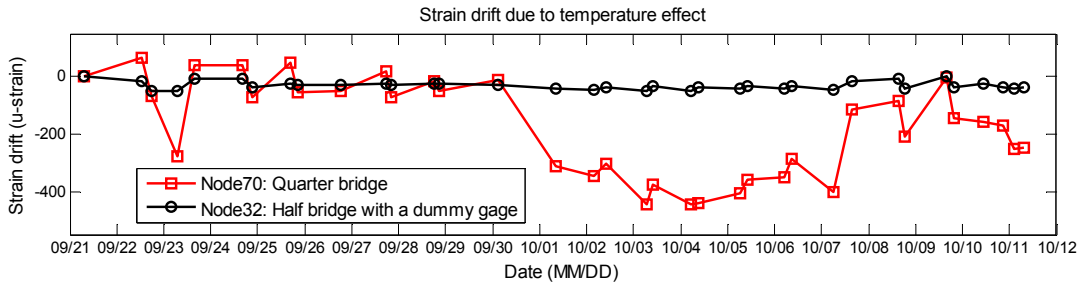

Fig. 16 Strain drifts due to temperature change over three weeks

The temperature compensation approach shows good performance, although some temperature effects are still present over the measurement period. These residual drifts may be attributed to the real effects of temperature change on structural strain responses or the different temperature sensitivities of resistors of 10~100 ppm comprising the Wheatstone bridge arms; further investigation will be required. However, if only dynamic strain measurements are of interest, the static strain drift due to temperature effect would not be an issue.

5.3 Strain sensing on the Jindo bridge girder

In addition to strain measurements on the pylon, strain sensing on the girder of the Jindo Bridge also has been carried out. In contrast to strain sensing on the pylon, the inside of the girder was not accessible for strain gage installation. To measure strain without peeling the paint, therefore, the friction-type magnet strain checker (FGMH-1) combined with the SHM-S board was used. Girder strains were measured at two different locations: one was on the bottom surface of the steel box girder at midspan of the bridge, and the other measurement was on the bottom surface of the girder around pylon bearing position as shown in Fig. 17. 25 Hz sampling rate and gain of 1001 times were used for this measurement.

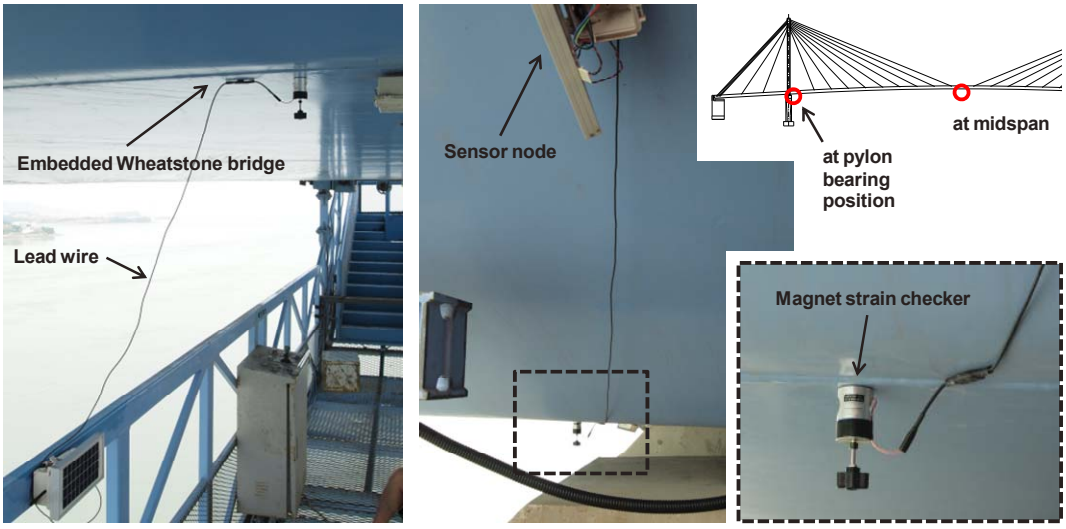

Fig. 17 Strain sensing on the girder using magnet strain checker with SHM-S board: at midspan (left), at pylon bearing position (middle) and close-up (right)

Fig. 18 shows the typical strain measurements on the girder subjected to traffic loading; several cars were passing the bridge at that time of the measurements, and the apparent peaks shown in the Fig. 18 may be attributed to the car traffic. The strain measurements at pylon bearing location (top of Fig. 18) and at midspan (bottom of Fig. 18) show clear differences. While the strain peaks in the pylon location measurement are downward, which means compression, however, the peaks in the midspan measurement are upward in tension direction. This is because the bottom surface of the steel box girder at the pylon bearing location is subjected to compressive force due to the negative bending moment when cars passing, and the bottom of the girder at midspan is in tension with positive bending.

The amplitudes of the peaks are quite different for the different sensing locations. The strain peak amplitudes are just 2~8 μstrain at the pylon bearing location, whereas they are 10~50 μstrain at midspan. Though the peak amplitudes vary depending on the car weight and speed, similar trends (i.e., higher amplitude strains at the midspan) were observed with other measurements; thus, the sensitivity of strain to traffic loading appears to be higher at midspan than at the pylon.

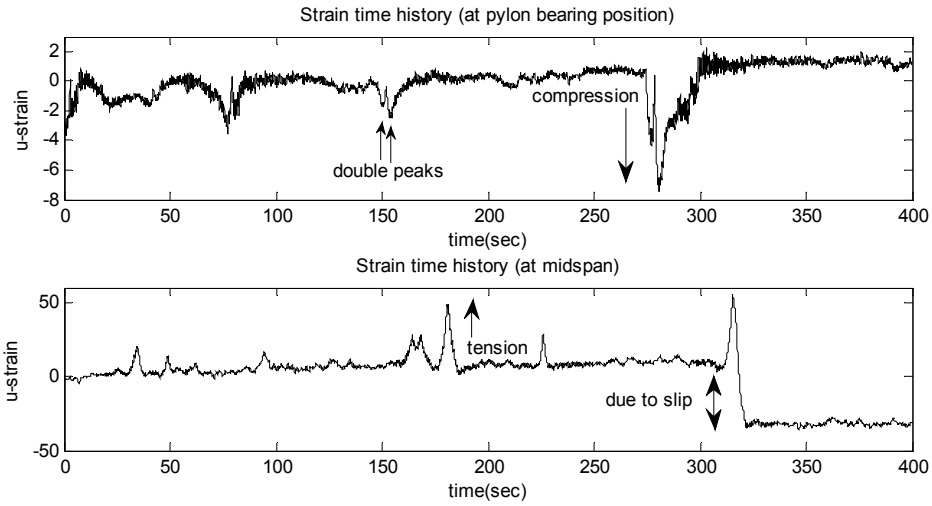

Fig. 18 Example strain measurements on the girder subjected to traffic loading: at pylon bearing location (top) and at midspan (bottom)

There was an abrupt signal drop after a high tension peak in the midspan strain measurement around 315 seconds (bottom of Fig. 18). This change may be attributed to the lateral slip of the magnet checker due to the heavy loading that caused a quite significant tension strain peak about 50 μstrain. Because the attractive force of the magnet is unidirectional perpendicular to the girder surface, the resistance to the lateral movement is relatively weak. Applying little silicon or clay dough around the strain checker would help to prevent the possible slippage.

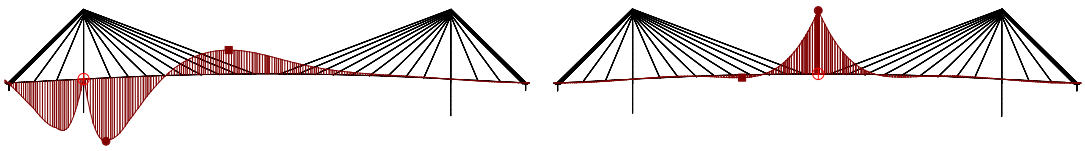

Fig. 19 Stress influence lines for girder bottom flange of the 2nd Jindo Bridge: at pylon bearing location (left) and at midspan (right)

Taking a close look at the strain peaks in the pylon location measurement, each set of compression peak is composed of two different-height peaks, which is not shown in the midspan strain measurement. For the peak around 75 seconds, a somewhat larger peak is appeared first then smaller peak follows (top of Fig. 18). In contrast, the peaks around 150 seconds and 280 seconds show a smaller peak first, followed by a larger peak. This phenomenon is caused by the double-concave shaped influence line for bending moment of multi-span continuous girder at

intermediate the support (see Fig. 19, left). Each of the double peaks occur when a car passing the lowest point of each of the concaves of the influence line. And if either-side span has different length, the double peaks may have different amplitudes.

6.Conclusions

In this paper, the development of wireless strain sensing system for Imote2 smart sensor platform and its application to the SHM of a cable-stayed bridge are investigated. The newly developed strain sensor board (SHM-S) and associated software (*SHMSAutoBalance*) are able to measure low-level ambient strain by precisely balancing the Wheatstone bridge, adjusting reference voltage of the instrumentation amplifier on the SHM-S board, and consequently obtaining up to 2507-times high gain. In addition to typical foil-type strain gage, the SHM-S board has been designed to accommodate a friction-type magnet strain sensor for ease of installation and measurement. The performances of the hardware and software have been validated with lab-scale tests, which showed comparable results with a conventional wired strain sensing system. A half-bridge configuration was used for temperature compensation using a dummy strain gage; a shunt calibration was also implemented on the SHM-S board. Moreover, because the board has been designed to be used with the ADC of the SHM-A board or SHM-DAQ board previously developed under ISHMP, it can fully utilize all the advantages of WSSN using ISHMP Services Toolsuite. Finally, the efficacy of the proposed system has been validated through field deployment on the 2nd Jindo Cable-Stayed Bridge in Korea. And the performance of the wireless strain sensing system for measurement of low-level ambient strain in a variable temperature environment was demonstrated.

Acknowledgements

This study is supported in part by the National Science Foundation Grant CMS09-28886 (Dr. S.C. Liu, program manager). And the support from Global Research Network program by the National Research Foundation in Korea (NRF-2008-220-D00117) is also gratefully acknowledged.

References

AAEON Technology Inc., (2008), "AEC-6905, Advanced embedded fanless controller with PCI and PC/104+ expansion", Taipei, Taiwan.

Bischoff, R., Meyer, J., Enochsson, O., Feltrin, G. and Elfgren, L. (2009), "Event-based strain monitoring on a railway bridge with a wireless sensor network", *Proceedings of the 4th International Conference on Structural Health Monitoring of Intelligent Infrastructure*, Zurich, Switzerland.

Cho, S., Jo, H., Jang, S.A., Park, J., Jung, H.J., Yun, C.B., Spencer, Jr., B.F. and Seo, J. (2010), "Structural health monitoring of a cable-stayed bridge using smart sensor technology: data analyses", *Smart Struct. Syst.*, **6**(5-6), 461-480.

Choi, H., Choi, S. and Cha, H. (2008), "Structural health monitoring system based on strain gauge enabled wireless sensor nodes," *Proceedings of the 5th International conference on networked sensing systems*.

Illinois Structural Health Monitoring Project (ISHMP) Service Toolsuite, http://shm.cs.uiuc.edu.

Jang, S.A., Jo, H., Cho, S., Mechitov, K.A., Rice, J.A., Sim, S.H., Jung, H.J., Yun, C.B., Spencer, Jr., B.F.

and Agha, G. (2010), "Structural health monitoring of a cable-stayed bridge using smart sensor technology: deployment and evaluation", *Smart Struct. Syst.*, **6**(5-6), 439-459.
Jo, H., Sim, S., Mechitov, K.A., Kim, R., Li, J., Moinzadeh, P., Spencer, B.F., Park, J., Cho, S., Jung, H., Yun, C., Rice, J.A. and Nagayama, T. (2011), "Hybrid wireless smart sensor network for full-scale structural health monitoring of a cable-stayed bridge", *Proceedings of the SPIE,* San Diego.
Kurata, M., Kim, J., Zhang, Y., Lynch, J.P., Linden, G.W., Jacob, V., Thometz, E., Hipley, P. and Sheng, L.H. (2010), "Long-term assessment of an autonomous wireless structural health monitoring system at the New Carquinez Suspension Birdge", *Proceedings of the SPIE,* San Diego.
MAXIM Inc. (2003), *MAX4194, Micropower precision instrumentation amplifier*, Sunnyvale, CA.
MAXIM Inc. (2006), *MAX5479, Dual-nonvolatile digital potentiometer*, Sunnyvale, CA.
MEMSIC (2006), *Imote2, Advanced wireless sensor network node platform*, Andover, MA.
MEMSIC (2007), *MICA2, Wireless measurement system*, Andover, MA.
Meyer, J., Bischoff, R., Feltrin, G. and Motavalli, M. (2010), "Wireless sensor networks for long-term structural health monitoring", *Smart Struct. Syst*., **6**(3), 263-275.
MicroStrain Inc. (2011), *SG-Link–mXRS, Wireless strain node*, Williston, VT.
MOTEIV (2006), *Tomote Sky, Ultra low power wireless sensor module*, San Francisco, CA.
Nagayama, T., Ruiz-Sandoval, M., Spencer, B.F., Mechitov, K.M. and Agha, G. (2004), "Wireless strain sensor development for civil infrastructure", *Proceedings of the 1st International Workshop on Networked Sensing Systems*, Tokyo, Japan.
National Instruments (2007a), *NI SCXI-1520, 8-Ch Universal strain gauge input module*, Austin, TX.
National Instruments (2007b), *NI SCXI-1314, Front-mounting Wheatstone bridge terminal block*, Austin, TX.
National Instruments (2011), *NI WSN-3214, 4ch strain gage node*, Austin, TX.
O'Brien, E., Znidaric, A. and Ojio, T. (2008), "Bridge weight-in-motion – latest developments and applications worldwide", *Proceedings of the International Conference on Heavy Vehicles, Heavy Vehicle Transport Technology and Weight-In-Motion*, Paris, France, 25-38.
O'connor, S., Kim, J., Lynch, J.P., Law, K.H. and Salvino, L. (2010), "Fatigue life monitoring of metallic structures by decentralized rainflow counting embedded in a wireless sensor network", *Proceedings of the ASME Conference on Smart Material, Adaptive Structure and Intelligent System,* Philadelphia.
Quickfilter Technologies, Inc. (2007), *QF4A512, 4-Ch programmable signal conditioner*, Allen, TX.
Rice, J.A. and Spencer, B.F. (2008), "Structural health monitoring sensor development for the Imote2 platform", *Proceedings of the SPIE,* San Diego.
Rice, J.A., Mechitov, K., Sim, S.H., Nagayama, T., Jang, S., Kim, R., Spencer, Jr., B.F., Agha, G. and Fujino, Y. (2010), "Flexible smart sensor framework for autonomous structural health monitoring", *Smart Struct. Syst.*, **6**(5-6), 423-438.
Spencer, B.F. and Cho, S. (2011), "Wireless smart sensor technology for monitoring civil infrastructure: technological developments and full-scale applications" , *Proceedings of the ASEM'11+,* Seoul, Korea.
Swartz, R.A., Jung, D., Lynch, J.P., Wang, Y. and Flynn, M. (2005), "Design of a wireless sensor for scalable distributed in-network computation in a structural health monitoring system", *Proceedings of the Int. Workshop on Structural Health Monitoring,* Stanford, CA.
Tokyo Sokki Kenkyujo Co., Ltd. (2005), *FGMH-1, Strain checker*, Tokyo, Japan.
Whelan, M.J. and Janoyan, K.D. (2009), "Design of a robust, high-rate wireless sensor network for static and dynamic structural monitoring", *J. Intell. Mater. Syst. Struct.*, **20**(7), 849-864.
Whelan, M.J., Gangone, M.V., Janoyan, K.D., Hoult, N.A., Middleton, C.R. and Soga, K. (2010), "Wireless operational modal analysis of a multi-span prestressed concrete bridge for structural identification", *Smart Struct. Syst.*, **6**(5-6), 579-594.
ZMD AG (2004), *ZMD31050, Advanced differential sensor signal conditioner*, Dresden, Germany.
Zonta, D., Wu, H., Pozzi, M., Zanon, P., Ceriotti, M., Mottola, L., Picco, G.P., Murphy, A.L., Guna, S. and Corra, M. (2010), "Wireless sensor networks for permanent health monitoring of historic buildings", *Smart Struct. Syst.*, **6**(5-6), 595-618.